A Parallel-Architecture Parametric Equalizer for Air-Coupled Capacitive Ultrasonic Transducers

Sean G. McSweeney, *Member IEEE*, and William M. D. Wright, *Senior Member IEEE*

***Abstract*—Parametric equalization is rarely applied to ultrasonic transducer systems, for which it could be used on either the transmitter or the receiver to achieve a desired response. An optimized equalizer with both bump and cut capabilities would be advantageous for ultrasonic systems in applications in which variations in the transducer performance or the properties of the propagating medium produce a less-than-desirable signal. Compensation for non-ideal transducer response could be achieved using equalization on a device-by-device basis. Additionally, calibration of ultrasonic systems in the field could be obtained by offline optimization of equalization coefficients.**

In this work, a parametric equalizer for ultrasonic applications has been developed using multiple bi-quadratic filter elements arranged in a novel parallel arrangement to increase the flexibility of the equalization. The equalizer was implemented on a programmable system-on-chip (PSOC) using a small number of parallel 4th-order infinite impulse response switched-capacitor band-pass filters. Because of the interdependency of the required coefficients for the switched capacitors, particle swarm optimization (PSO) was used to determine the optimum values. The response of a through-transmission system using air-coupled capacitive ultrasonic transducers was then equalized to idealized Hamming function or brick-wall frequency-domain responses. In each case, there was excellent agreement between the equalized signals and the theoretical model, and the fidelity of the time-domain response was maintained. The bandwidth and center frequency response of the system were significantly improved. It was also shown that the equalizer could be used on either the transmitter or the receiver, and the system could compensate for the effects of transmitter-receiver misalignment.

I. Introduction

Capacitive ultrasonic transducers [1] have seen much recent interest as alternatives to piezoelectric transducers, particularly for applications of ultrasound in air and other gases [2], because they do not require impedance matching layers and tend to be broadband and highly efficient. A capacitive ultrasonic transducer is essentially a parallel plate capacitor, with one fixed rigid electrode (the backplate) and one movable flexible electrode (the membrane), with a thin air gap or cavity in between. Typically, a dc bias voltage is applied between the two electrodes to build up charge between them. When operating as a transmitter, a superimposed voltage oscillating at the desired ultrasonic frequency causes the charge between the two electrodes to vary, and displaces the membrane to generate ultrasound; similarly, when operating as a receiver, an ultrasonic wave striking the membrane causes it to displace, and produces a detectable change in charge between the membrane and backplate. The thickness (and mass) of the membrane, and the surface profile of the backplate usually dictate the frequency response and the sensitivity of the device.

The center frequencies of capacitive ultrasonic transducers operating in air typically range from a few tens of kilohertz up to the low megahertz regime, depending on the method of device construction. The backplates for low-frequency devices are usually grooved by various conventional machining methods [3], whereas those for the higher-frequency devices may be mechanically roughened or polished [4], have ridges deposited on a smooth conducting surface [5], or have various patterns of pits etched into them [6]. The membrane is typically a separate metalized dielectric polymer film such as polyethylene terephthalate (PET) or polyimide, with a thickness ranging from about 2 to 25 μm, placed over the backplate.

The application of capacitive ultrasonic transducers has been somewhat limited, primarily because of the lack of repeatability between devices, mainly resulting from the methods of production of the backplates but also resulting from assembly using a separate membrane. This, of course, led to the development of capacitive micromachined ultrasonic transducers (CMUTs) in their various forms [7]–[11], in which the backplate and front plate [12] are manufactured together in the same photolithographic process, typically involving a sacrificial etch to produce the electrode cavity, allowing much tighter control of the device dimensions and improved repeatability between devices.

However, for applications in air, CMUTs have some significant limitations. CMUTs tend to have small sealed cavities that are only a few tens of microns in diameter, leading to very resonant devices, even when the cavities are interconnected [10]. The production of larger-area individual CMUTs is more challenging and requires tight control of the residual stresses, but has produced devices with improved bandwidth [11]. In addition, the choice of CMUT front plate material is usually limited to those that are compatible with the photolithographic manufacturing process, although hybrid devices with separate titanium foil front plates have been produced [13]. Air-coupled ap-

Manuscript received June 17, 2011; accepted October 28, 2011. This work was supported by a Government of Ireland Postgraduate Research Scholarship from the Irish Research Council for Science, Engineering and Technology (IRCSET).

The authors are with the Department of Electrical and Electronic Engineering, University College Cork, Ireland (e-mail: bill.wright@ucc.ie).

Digital Object Identifier 10.1109/TUFFC.2012.2159

plications typically require devices with active areas of a few square millimeters or greater, meaning that most CMUTs for operation in air consist of arrays of many small elements [14]. However, there have been significant advances made in device fabrication techniques, with direct wafer-bonded large-area single-element devices being developed [15], and the manufacturing variability of such devices is likely to be significantly less than conventional capacitive ultrasonic transducers.

The work described in this paper investigated the use of a parametric equalizer to selectively modify the response of capacitive ultrasonic transducers to produce a desired output or improve performance. Equalization filtering [16] is well established for audio channel compensation, and has been explored previously for ultrasonic systems [17]. Typical equalizers consist of several different filter circuits connected in series, with each individual filter influencing a specific frequency range and modifying the signal in sequence.

The use of standard active electronic components such as digitally programmable capacitors and resistors in these equalizer circuits is a less attractive proposal than an equalizer that has potential for miniaturization onto an integrated circuit. An equalizer constructed using switched capacitor (SC) architecture and leveraging recent advances in optimization would be a more useful technology for ultrasonic systems in general, and could be integrated with a CMUT into a single package. SC filters are often used in audio applications [18], and they have also been applied to the RF spectrum [19] and for video application [20]. Additionally, very large scale integration (VLSI) implementations of these filters have been detailed [21], highlighting their ease of use, and their application as equalizers is well understood [22]. There seems to have been no attempt to apply this technology to ultrasonic equalizer systems.

The work described here has developed a parametric equalizer for ultrasonic applications, using multiple bi-quadratic SC filter elements, arranged in a novel parallel configuration. This arrangement gives significant advances over the more conventional series arrangement because it allows more flexible equalization, and potential power savings because elements that are not required may be switched off. However, one of the key challenges in implementing multiple SC filter elements in a parallel architecture is the interdependency of the SC parameters required to produce a desired response. Many parameters are indirectly coupled to each other such that, for example, optimizing the equalizer to deliver a particular magnitude response may then have detrimental consequences for the frequency response. Hence, the selection of a suitable set of optimized parameters for the equalizer is an ill-posed inverse problem, which is in itself still an area of considerable research [23]. To maximize the versatility of the equalizer, a particle swarm optimization (PSO) technique was used to determine the optimum set of parameters for several specific applications. The desired transducer response is specified, in either the time domain or the frequency domain, and the PSO algorithm determines the optimum set of SC parameters that minimizes the error between the measured response and the desired response.

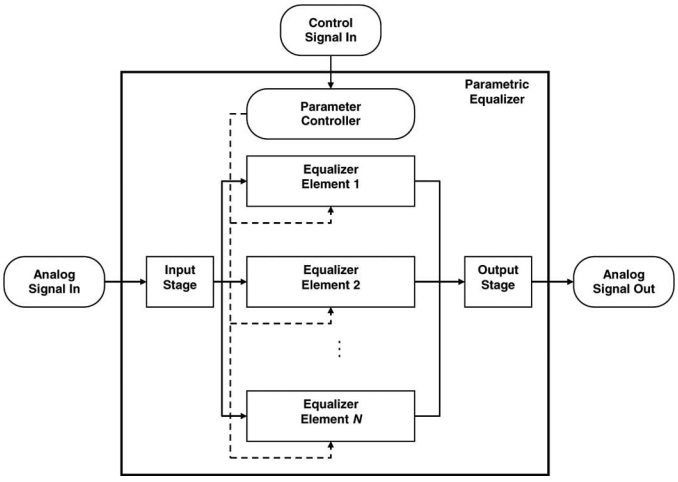

Fig. 1. Schematic diagram of the parallel architecture parametric equalizer.

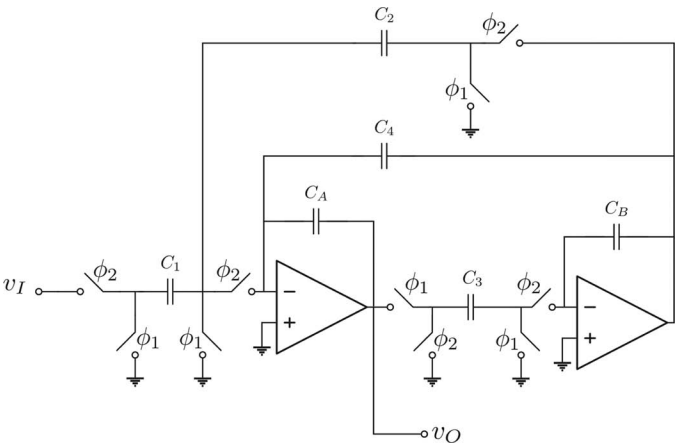

Fig. 2. Schematic diagram of an individual switched capacitor (SC) bi-quadratic bandpass filter.

II. The Equalizer Architecture

The equalizer architecture has been described in considerable detail elsewhere [24], [25], but in general terms it consists of N equalizer elements arranged in parallel as shown schematically in Fig. 1, with each equalizer element containing an oscillator-controlled, SC bi-quadratic filter circuit shown in Fig. 2. In the current work, a parametric equalizer with $N = 2$, 4, or 6 is described, although in principle a larger number of parallel elements may be used. Each element forms a 4th-order biquadratic bandpass filter, and by combining the elements in parallel rather than in series, almost all filter types may be developed with a sufficient number of elements to give significant levels of equalization. Unlike a series arrangement, individual elements may be switched on or off as required, resulting

in significant power savings. The parameter control provides parameter signals to the clock generator, the SC parameters for the bi-quadratic filters, and also includes the I/O and rail gating circuitry. The input and output stages consist of impedance matching, biasing, voltage regulation, and other circuitry, to boost the equalized signals to the voltages required by the transducers.

Many of the required parameters are indirectly coupled to each other. To determine the optimum set of parameters in the current work, particle swarm optimization (PSO) was used, which is a stochastic optimization technique that is a subset of the biologically inspired computation family of algorithms [26]. This method was originally developed in attempts to model the behavior of flocks of birds and schools of fish [27] and has the property of emergence in its computation. Local minima trapping is also less prevalent in PSO in comparison to other algorithms [28].

In essence, PSO consists of a predefined number (the swarm) of solution candidates (the particles) moving around the solution hyperspace (cost function) that contain both positional and velocity vectors that are a function of the swarm best, the particle best, and the previous values. After a predefined number of epochs (cycles of the algorithm) or a certain resolution in error estimate, the best particle is chosen as the minimum value.

A Euclidean distance measure is then calculated for each point in the localized solution space from the minimization value. This calculation ensures that invalid points (i.e., ones that would return values outside the required range) are not obtained, and a weighting is given to the importance of each parameter. From this distance measure, the appropriate minimum point is returned for each bi-quadratic element parameter, and a matrix of the parameter values is obtained for the closest match possible for a particular desired minimum value.

III. Modeling

The output of the parametric equalizer was modeled in MATLAB (The MathWorks, Natick, MA) using the unmodified time-domain response of the ultrasonic through-transmission system. Because the filter structure in this work is parallel biquadratic-type, the sampled time transfer function $H_i(z)$ of individual 2nd-order sections may be given by

$$H_i(z) = \frac{a_0 + a_1 z^{-1}}{b_0 + b_1 z^{-1} + b_2 z^{-2}}, \tag{1}$$

where a and b are numerator and denominator coefficients, respectively. These coefficients are defined in terms of the switching capacitors shown in Fig. 2 as

$$\begin{aligned} a_0 &= C_1 C_\mathrm{B} \\ a_1 &= -C_1 C_\mathrm{B} \end{aligned} \tag{2}$$

and

$$\begin{aligned} b_0 &= C_\mathrm{A} C_\mathrm{B} \\ b_1 &= C_3 C_4 - C_2 C_3 - 2C_\mathrm{A} C_\mathrm{B} \\ b_2 &= C_\mathrm{A} C_\mathrm{B} - C_3 C_4. \end{aligned} \tag{3}$$

Each parallel element of the system has two biquad sections cascaded with input and output programmable gain amplifiers (PGAs). Thus, the system transfer function of the parallel 4th-order biquadratic sections for the architecture of filter shown in Fig. 2 is given by

$$H(z) = \sum_{i=0}^{K} G_{i1} H_{i1}(z) H_{i2}(z) G_{i2}, \tag{4}$$

where G_{i1} and G_{i2} are the gains of the PGAs and H_{i1} and H_{i2} are the transfer functions of each individual 2nd-order section in the ith element. The optimal approximation of the filter coefficients for the dial-in resolution of the circuitry are obtained from the approximation method described in Section II. For the purposes of this work, the equalizer was used to obtain a desired frequency-domain response $Y(w)$, to which the obtained frequency-domain response $X(w)$ is minimized. More formally, the particle cost Ω is mean squared error (MSE)-based, with

$$\Omega = \frac{1}{N} \sum_{w=w_1}^{w_2} (Y(w) - X(w))^2, \tag{5}$$

where N is the number of frequency buckets between w_1 and w_2. This method could also be used, in principle, to obtain a desired time-domain response, although this is outside the scope of the current study. The pulse shape was modified using a Bessel-based equalizer, which is well known to maintain the best pulse fidelity in infinite impulse response (IIR) filters [29].

IV. Experimental Implementation

An equalizer with 2, 4, or 6 parallel elements was implemented on an array of CY8C29466 programmable systems-on-chips (PSOCs) from Cypress Semiconductor Corp. (San Jose, CA) and used to manipulate the response of a pair of capacitive ultrasonic transducers operating in air. A schematic of the experimental apparatus is shown in Fig. 3. A TG1010 arbitrary waveform generator (AWG) from Thurlby Thandar Instruments Ltd. (Huntingdon, UK) was used to produce a standard impulse (a single square pulse of 20 μs duration and 1 V amplitude) which then passed through the parametric equalizer and was then amplified to 20 V and superimposed over a 20 V dc bias before reaching the transmitting Senscomp 600 capacitive ultrasonic transducer (SensComp Inc., Livonia, MI), with a nominal center frequency of 50 kHz and −3-dB bandwidth of 25 kHz (50%).

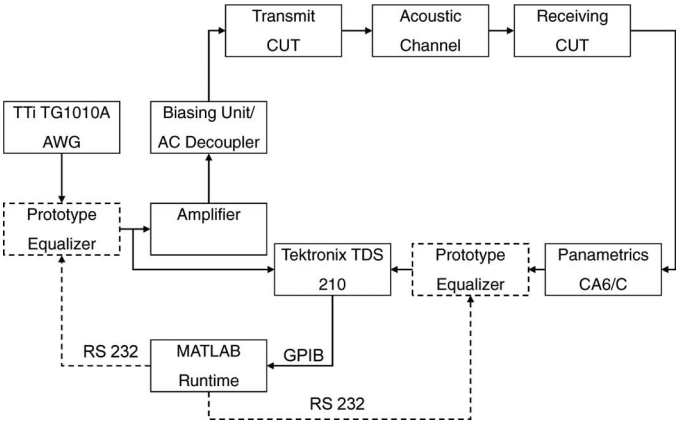

Fig. 3. Schematic diagram of experimental apparatus.

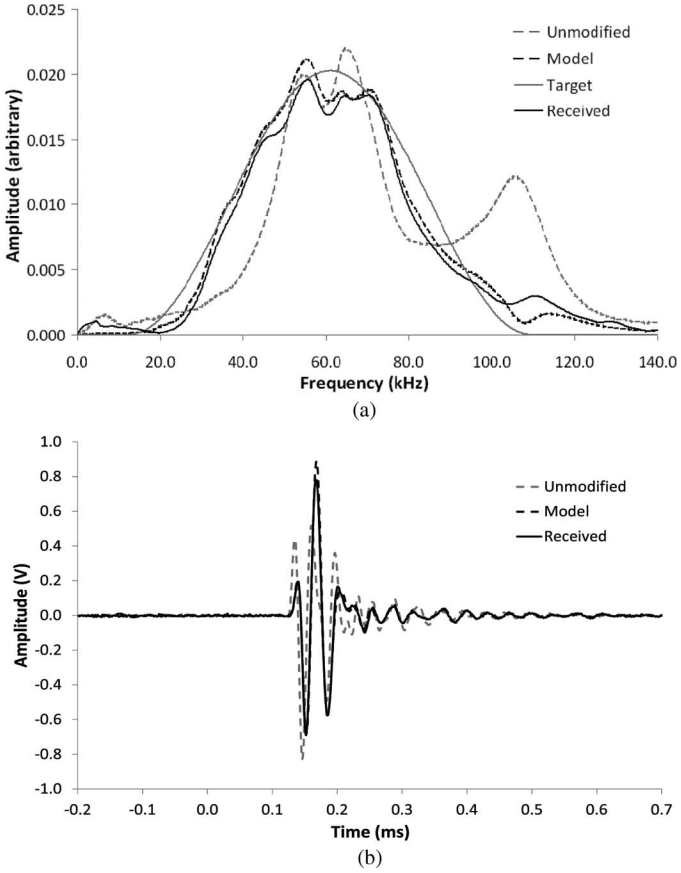

Fig. 4. Smoothing the frequency response to a Hamming function centered at 60 kHz, showing (a) the frequency response and (b) the corresponding time-domain waveforms.

After propagating through the air gap of 21.5 cm, the ultrasound was detected by either another Senscomp 600 device, or a broadband capacitive ultrasonic transducer with a polished backplate and a 12-μm metalized PET membrane, which has been shown in previous work [30] to have a center frequency of 180 kHz and a −3-dB bandwidth of 100%. The received signals were then decoupled from the 100 V dc receiver bias and amplified using a CA6/C charge-sensitive amplifier (Panametrics NDT, Waltham, MA), digitized on a TDS210 oscilloscope (Tektronix, Beaverton, OR) and transferred to a PC via a GPIB interface for analysis and parameter selection. The PSO minimization was run in MATLAB [31], using the Clerc PSO function [32].

The optimum SC values for the parametric equalizer were determined as follows: First, an unmodified impulse response was transmitted through the air gap to determine the ultrasonic response of the system before equalization, and to provide the PSO algorithm with an initial signal and set of parameter values. The desired set point or response, for example, a target frequency spectrum such as a brick wall between 20 and 100 kHz, was then fed into the PSO algorithm. The algorithm then determined the optimum SC parameters (dial-in values) by minimizing the cost function between the actual response and the desired response. These parameters were then dialed-in through a COM (RS-232) port, equalizing the ultrasonic channel. When the parametric equalizer received the dial-in values through the COM interface, it initially gathered and then sorted these parameters. The equalizer then performed a check on the values received for validity before the parameters were dialed into the appropriate counters (used as the clocks) and the required bi-quadratic equalizer blocks.

V. Results

Several experiments were performed to illustrate the capabilities of the parametric equalizer in obtaining a desired or idealized response from a capacitive ultrasonic transducer, and manipulating the center frequency and −3-dB bandwidth of the transducer output or received signal. In these experiments, an equalizer with six parallel elements was used, and the same transient impulse from the AWG was used in all experiments. Sixteen signal averages were used, unless stated otherwise. Great care was taken to ensure that all other parameters (path length, air temperature etc.) were identical in all tests.

A. Idealizing the Response

A pair of Senscomp 600 capacitive ultrasonic transducers with nominal diameters of 38.4 mm and center frequencies of 50 kHz were used in the through-transmission system shown in Fig. 3. The unmodified frequency response of the transducer pair is given by the dashed gray line in Fig. 4(a) and shows resonances at 55, 64, and 104 kHz. The parametric equalizer with six elements in parallel was then connected to the transmitter used to equalize the output to a more idealized response, which was a simple Hamming function in the Fourier domain, between upper and lower −3-dB limits of 40 and 80 kHz and centered at 60 kHz. The PSO algorithm selected the required dial-in parameters for the SC equalizer elements. The frequency spectra are shown in Fig. 4(a), with the corresponding received ultrasonic waveforms overlaid in Fig. 4(b). It can be seen that the received signal is a close match to the Hamming target, with the 104-kHz peak

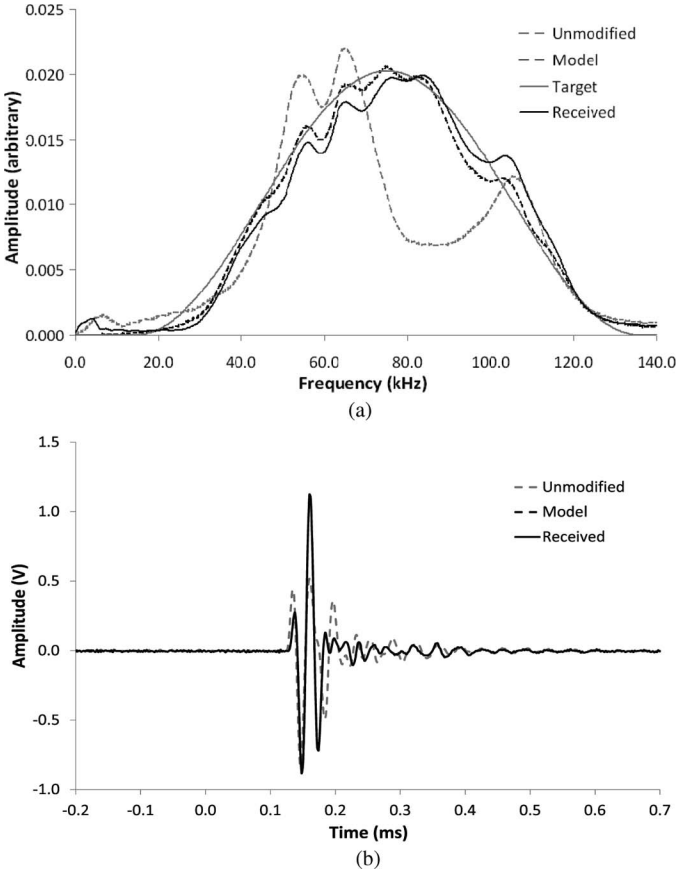

Fig. 5. Shifting the frequency response to a Hamming function centered at 75 kHz, showing (a) the frequency response and (b) the corresponding time-domain waveforms.

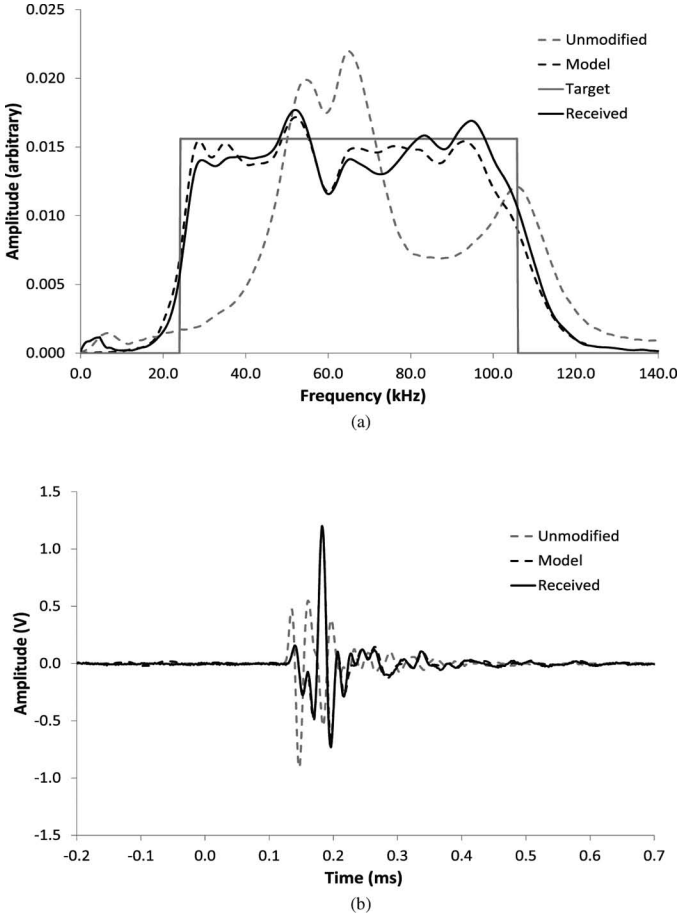

Fig. 6. Extending the bandwidth to a brick-wall or top-hat function in the frequency domain between 25 and 105 kHz, showing (a) the frequency response and (b) the corresponding time-domain waveforms.

completely removed and a significant reduction in the 64-kHz peak, giving a much smoother response. The −3-dB bandwidth has also been extended from 25.9 to 38.2 kHz, which is an increase of more than 47%. It can also be seen that the modeled response is an excellent match to the received response in the frequency domain.

B. Shifting the Center Frequency

The same transducer was then equalized to an idealized Hamming target response in the frequency domain where the nominal center frequency was increased from 60 to 75 kHz. As before, this target response was used by the PSO to determine the optimum dial-in parameters. The frequency spectra are shown overlaid in Fig. 5(a), with the corresponding received ultrasonic waveforms overlaid in Fig. 5(b). It can be seen again that the received transducer response in the frequency domain closely matches the idealized target response and the model prediction, with the shift in center frequency clearly visible. The overall response between 50 and 110 kHz has been significantly smoothed, with only minor ripple in the spectrum; this is a function of the number of parallel equalizer elements used. Of particular note is the change in −3-dB bandwidth from 25.9 kHz in the unmodified response to 54.4 kHz in the equalized response, an increase of 110%. This is reflected in the time-domain waveforms shown in Fig. 5(b), with a corresponding reduction in ringing, shorter pulse duration, and no detrimental phase delay. Again, the correlation between the received signal and the theoretical prediction is excellent.

C. Extending the Bandwidth

In principle, nearly any appropriately-shaped target function in the frequency domain may be used, so to test the limits of the parametric equalizer further, the same transducer was equalized to an idealized response in the frequency domain in which the desired spectrum was a brick wall between 25 and 105 kHz, which is approaching the physical limits of the transducer. The frequency spectra are shown in Fig. 6(a), with the corresponding received ultrasonic waveforms overlaid in Fig. 6(b). It can be seen that the bandwidth of the transducer response has been successfully extended, and that there is a good match with the target brick-wall target function, although there is still some ripple in the passband that corresponds to the poles of the six equalizer elements used. These are now spread out over a wider frequency range, and the levels of boost required between 20 and 50 kHz and 70 and 100 kHz are skewing the equalization. The signal in the time domain clearly has a higher frequency content with a significantly

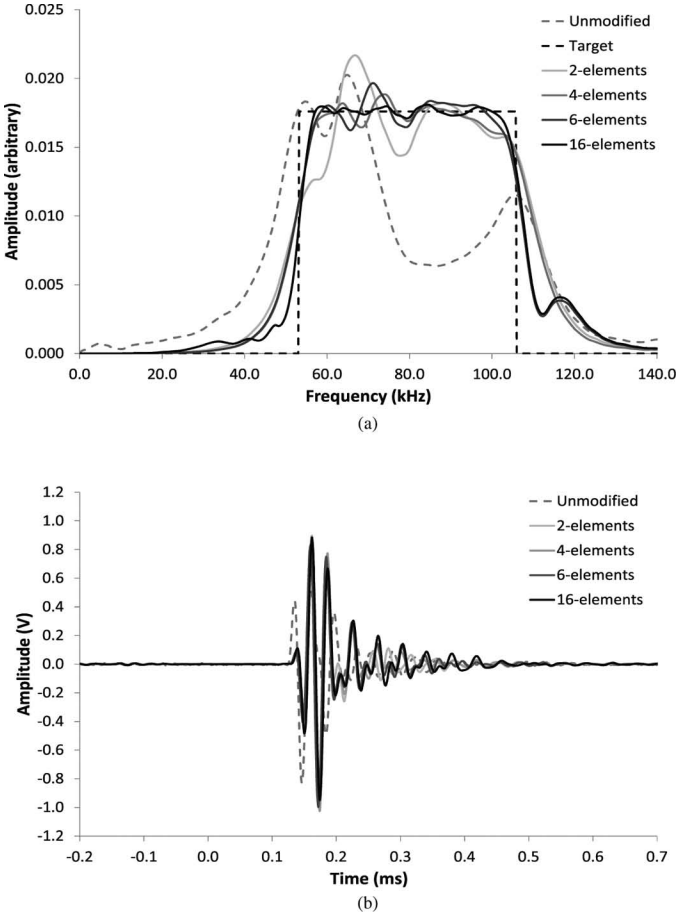

Fig. 7. Increasing the number of parallel equalizer elements from 2 to 16, showing (a) the modeled frequency responses and (b) the corresponding modeled time-domain waveforms.

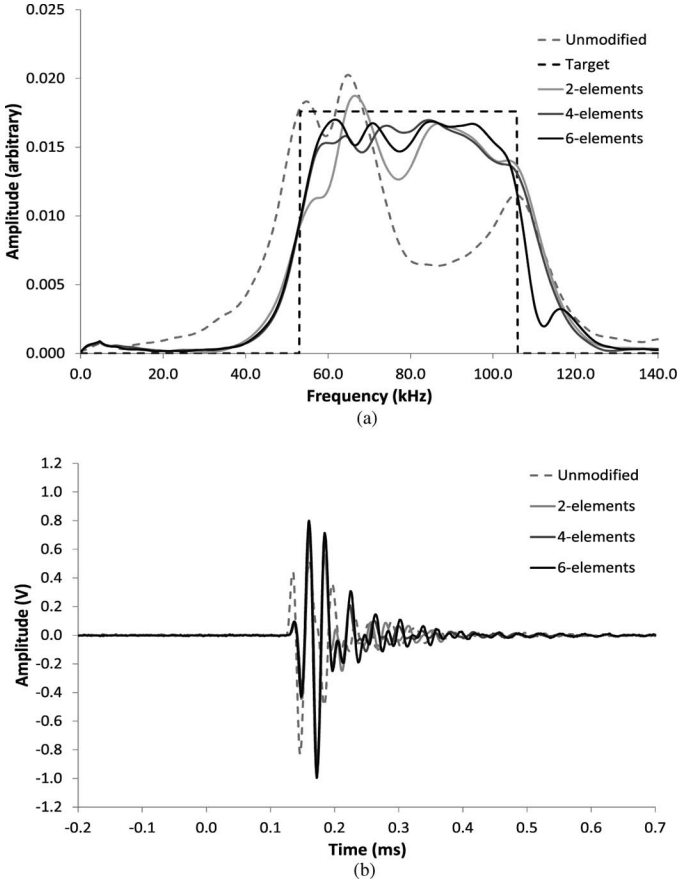

Fig. 8. Increasing the number of parallel equalizer elements from 2 to 6, showing (a) the received frequency responses and (b) the corresponding time-domain waveforms.

changed pulse shape, as would be expected, and again there is excellent correlation with the theoretical model.

D. Increasing the Number of Elements

It is clear from the results shown so far that the number of elements used in the equalizer dictates the degree of flexibility and the level of equalization that can be obtained. The number of equalizer elements used was varied, with parallel configurations using 2, 4, 6, and 16 elements being considered. The response of each equalizer was first modeled for an idealized brick-wall target response between 53 and 106 kHz; the theoretical frequency spectra are shown in Fig. 7(a), with the corresponding ultrasonic waveforms overlaid in Fig. 7(b). It is clear that with an increasing number of parallel elements, the theoretical response more closely approximates the target function, with very little passband ripple occurring with the 16-element equalizer. The received frequency domain and time-domain responses from the 2-, 4-, and 6-element equalizers are shown, respectively, in Fig. 8(a) and Fig. 8(b). The 16-element equalizer was not implemented in this study because this would have required a significant amount of additional PSOC hardware that was unavailable. However, it is clear that the received and modeled responses in both the time and frequency domains are excellent matches, and that the 16-element equalizer response should correspond in a similar fashion.

E. Higher-Frequency Operation With Misalignment

Another series of experiments was conducted to test the equalizer with a different capacitive ultrasonic transducer operating at a higher frequency. The same Senscomp 600 device used in previous experiments was used as the transmitter, but the Senscomp 600 receiver was replaced with a broadband capacitive ultrasonic transducer with a polished backplate and a 12-μm metalized PET membrane. This receiver had a center frequency of 180 kHz with a 100% bandwidth, thus the equalizer could be used to modify the response of a device at higher frequencies. In this set of experiments, the equalizer was attached to the receiver instead of the transmitter. Because of the size of the switched capacitors available in the PSOC implementation of the equalizer, the upper frequency range was limited to approximately 150 kHz. With a 1.5-MHz clock this represents an over sampling ratio of 10, which is at the lower limit for sampled analog systems. The response of the system can be seen in Fig. 9(a), and the corresponding frequency spectra in Fig. 9(b). The initial on-axis response

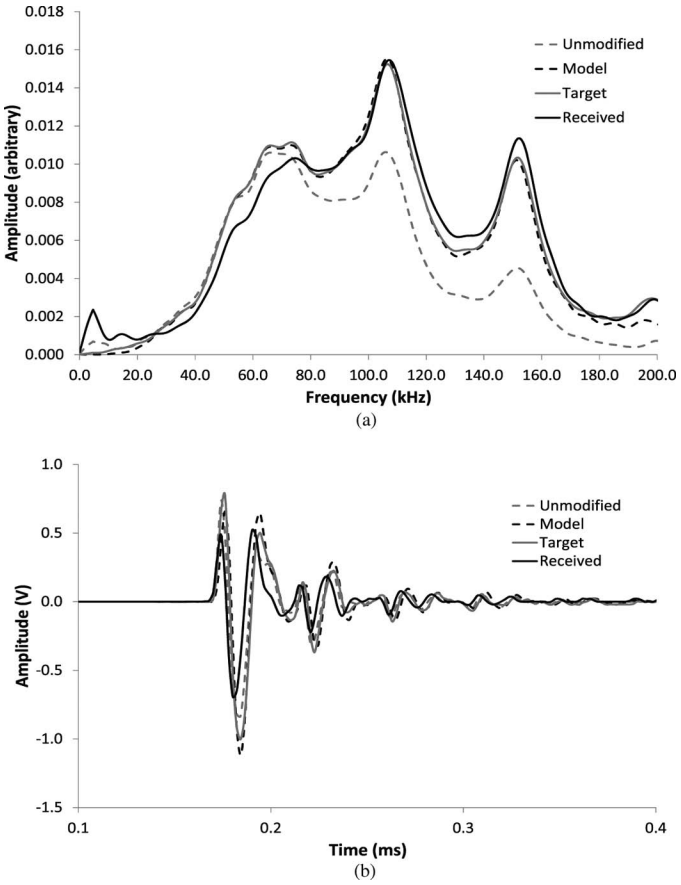

Fig. 9. Modifying the frequency response of a higher frequency transducer, showing (a) the frequency response and (b) the corresponding time-domain waveforms.

formed the target response for the optimization. The capacitive ultrasonic transducer receiver was then rotated by 10° about a vertical axis through its front face, i.e., the transducer separation was unchanged and the center of the receiver was still in the center of the on-axis beam from the Senscomp transmitter, but the normals to the receiver and transmitter faces were no longer coincident; this is representative of a common misalignment problem in through-transmission systems. The received (unmodified) response from the misaligned system is also shown in Fig. 9(a), and Fig. 9(b) shows that the frequency content of the impulse response has been changed, as expected. PSO optimization for an equalization of this unmodified response to the original target response produced the modeled and received results shown in Fig. 9(a) and Fig. 9(b). Again, there is good correlation between theory and experiment.

VI. Discussion

The impulse response results as reported in Section V for all cases have shown that significant modification of the usable frequency spectrum of an ultrasonic system is possible with low-order parallel filter elements using PSO without affecting the critical parameters of the impulse response. The time-domain waveforms show little or no phase delay in the equalized signal; this is due to the use of Bessel filters for the individual equalizer sections, which helps to maintain pulse fidelity and avoid long ringing times for these sections. The received equalized pulses had less ringing than the unmodified signals, corresponding to the increase in bandwidth, and the correlation with the model prediction in the time domain is also excellent. The variation in pulse arrival time is similarly negligible between the modified and unmodified results; this is one distinct advantage of a sampled analog equalization system over a digital equalization system, in which conversion times from analog to digital, processing, and conversion back to analog can sometimes result in a significant and unacceptable delay.

With frequency sampling points at approximately 250 Hz intervals up to 140 kHz, the MSE as defined in (3) for the 60-kHz Hamming target function presented in Section V-A ranges between 2.2×10^{-5} for the case of the unmodified response and 3×10^{-6} for the received equalized signal. The potential improvement in the obtained error with an increased number of parallel elements, if this is required for the design, can be seen with the error from the simulated 25 to 105 kHz brick-wall target function shown in Section V-D, where the MSE obtained for 2-, 4-, 6-, and 16-element designs are 13×10^{-6}, 9.6×10^{-6}, 6.6×10^{-6}, and 5.35×10^{-6}. It should be noted that the brick-wall target is much more difficult to achieve than the simpler Hamming target. As expected, diminishing error gains are obtained with increasing order, and most of the equalization can be achieved with low-order filters for systems that are insensitive to minor passband ripple. The transducer misalignment in Section V-E is just a representative example of how the equalizer may be used to compensate for minor differences in performance that could also, for example, occur between two nominally identical devices as a result of variability in their manufacturing processes. There is a slight increase in divergence between the modeled and received results when using the higher-frequency transducer; this is most likely due to a combination of spatial effects, aliasing, non-linearities, and the higher-frequency limitations of the PSOC, and will be investigated further.

The benefit of using a parallel architecture for parametric equalization cannot be overstated, and the method is compact and may be easily integrated into sensor front-ends. However there is a price for this enhanced capability, which is, in addition to increased system complexity, an increase in the power usage of the front-end electronics. As with all SC-based systems, there is a certain level of substrate noise coupling that is determined by the architecture, switching frequency, signal power, and filter parameters. This must also be accounted for in the design of any equalizer system, especially when real-time processing is required.

Care must also be taken when choosing an appropriate sampling frequency which, for SC circuits, must usually be at least 5 times the Nyquist rate. The noise generated by each switching element is approximately white noise,

and is distributed from 0 Hz to the Nyquist sampling rate. When equalizing a broadband transducer, if the switching frequency is not high enough, there may be more noise introduced within the transducer passband, in which case the dynamic range will be reduced.

Although this method has been applied to a capacitive ultrasonic transducer through-transmission system, the principles of this work are valid for many different types of transducer and arrangements in which there is a wideband response with peak-to-trough frequency domain levels within the dynamic range of the system.

VII. Conclusions

The details of a novel parallel-architecture biquadratic switched capacitor parametric equalization system utilizing PSO minimization to optimally match a desired frequency-domain response have been presented. It has been shown that for ultrasonic transducer systems, optimized switched capacitor parametric equalization may be used to compensate for undesirable responses in the frequency domain, and thus maintain a desired signal across a bandwidth of interest, so long as the modification required is within the physical capabilities of the transducer system. The principles of this work are valid for many transducer arrangements where there is a wideband response with peak to trough frequency domain levels within the dynamic range of the system. Future work will include an investigation into real-time equalization, the use of additional equalizer elements, and alternative optimization algorithms.

References

[1] M. Rafiq and C. Wykes, "The performance of capacitive ultrasonic transducers using v-grooved backplates," *Meas. Sci. Technol.*, vol. 2, no. 2, pp. 168–174, 1991.

[2] A. Gachagan, G. Hayward, S. P. Kelly, and W. Galbraith, "Characterization of air coupled transducers," *IEEE Trans. Ultrason. Ferroelectr. Freq. Contr.*, vol. 43, no. 4, pp. 678–689, Jul. 1996.

[3] J. Hietanen, P. Mattila, F. Tzusiki, H. Vaatitja, and M. Luukkala, "Factors affecting the sensitivity of electrostatic ultrasonic transducers," *Meas. Sci. Technol.*, vol. 4, no. 10, pp. 1138–1142, 1993.

[4] H. Carr and C. Wykes, "Diagnostic measurements in capacitive transducers," *Ultrasonics*, vol. 31, no. 1, pp. 13–20, 1993.

[5] M. J. Anderson, J. A. Hill, C. M. Fortunko, N. S. Dogan, and R. D. Moore, "Broadband electrostatic transducers: Modelling and experiments," *J. Acoust. Soc. Am.*, vol. 97, no. 1, pp. 262–272, 1995.

[6] D. W. Schindel, D. A. Hutchins, L. Zou, and M. Sayer, "The design and characterization of micromachined air-coupled capacitance transducers," *IEEE Trans. Ultrason. Ferroelectr. Freq. Contr.*, vol. 42, no. 1, pp. 42–50, Jan. 1995.

[7] M. I. Haller and B. T. Khuri-Yakub, "A surface micromachined electrostatic ultrasonic air transducer," in *Proc. IEEE Ultrasonics Symp.*, 1994, pp. 1241–1244.

[8] A. S. Ergun, Y. Huang, X. Zhuang, O. Oralkan, G. G. Yaraholu, and B. T. Khuri-Yakub, "Capacitive micromachined ultrasonic transducers: Fabrication technology," *IEEE Trans. Ultrason. Ferroelectr. Freq. Control*, vol. 52, no. 12, pp. 2242–2258, 2005.

[9] P.-C. Eccardt, K. Niederer, T. Scheiter, and C. Hierold, "Surface micromachined ultrasonic transducers in CMOS technology," in *Proc. IEEE Ultrasonics Symp.*, 1996, pp. 959–962.

[10] G. Caliano, F. Galanello, A. Caronti, R. Carotenuto, and M. Pappalardo, "Micromachined ultrasonic transducers using silicon nitride membrane fabricated in PECVD technology," in *Proc. IEEE Ultrason. Symp.*, 2000, pp. 963–967.

[11] J. S. McIntosh, D. A. Hutchins, D. R. Billson, T. J. Robertson, R. A. Noble, and A.D. R. Jones, "The characterization of capacitive micromachined ultrasonic transducers in air," *Ultrasonics*, vol. 40, no. 1–8, pp. 477–483, May 2002.

[12] M. Kupnik, I. O. Wygant, and B. T. Khuri-Yakub, "Finite element analysis of stress stiffening effects in CMUTS," in *Proc. IEEE Ultrasonics Symp.*, 2008, pp. 487–490.

[13] M. Kupnik, P. O'Leary, A. Schroder, and I. Rungger, "Numerical simulation of ultrasonic transit-time flowmeter performance in high temperature gas flows" in *Proc. IEEE Ultrasonics Symp.*, 2003, vol. 2, pp. 1354–1359.

[14] J. S. McIntosh, D. A. Hutchins, G. Etcheverry, D. R. Billson, R. A. Noble, R. R. Davies, and L. Koker, "Micromachined capacitive transducer array for imaging in air," in *Proc. IEEE Ultrasonics Symp.*, 2001, pp. 929–932.

[15] I. O. Wygant, M. Kupnik, J. C. Windsor, W. M. Wright, M. S. Wochner, G. G. Yaralioglu, M. F. Hamilton, and B. T. Khuri-Yakub, "50 kHz capacitive micromachined ultrasonic transducers for generation of highly directional sound with parametric arrays," *IEEE Trans. Ultrason. Ferroelectr. Freq. Control*, vol. 56, no. 1, pp. 193–203, 2009.

[16] S. J. Orfanidis, "High-order digital parametric equalizer design," *J. Audio Eng. Soc.*, vol. 53, no. 11, pp. 1026–1046, 2005.

[17] J. Andersen and L. Wilkins, "The design of optimum lumped broadband equalizers for ultrasonic transducers," in *Proc. IEEE Ultrasonics Symp.*, 1977, pp. 422–427.

[18] R. Perez-Aloe, J. F. Duque-Carrillo, E. Sanchez-Sinencio, J. M. Valverde, G. Torelli, A. H. Reyes, and F. Maloberti, "Programmable time-multiplexed switched-capacitor variable equalizer for arbitrary frequency response realizations," *IEEE J. Solid-state Circuits*, vol. 32, no. 2, pp. 274–278, 1997.

[19] U.-K. Moon, "CMOS high-frequency switched-capacitor filters for telecommunication applications," *IEEE J. Solid-state Circuits*, vol. 35, no. 2, pp. 212–220, 2000.

[20] K. W. H. Ng, S. L. Vincent, C. Luong and H. Luong, "A 3-V 44-MHz. switched-capacitor band-pass filter for digital video application," in *Proc. IEEE Int. Symp. Circuits and Systems*, 2002, vol. 4, pp. 627–630.

[21] K. Wong, K. H. Abed, and S. B. Nerurkar, "VLSI implementations of switched capacitor filter," in *Proc. IEEE SoutheastCon*, 2005, pp. 29–33.

[22] J. F. Duque-Carrillo, J. Silva-Martinez, and E. Sanchez-Sinencio, "Programmable switched-capacitor bump equalizer architecture," *IEEE J. Solid-state Circuits*, vol. 25, no. 4, pp. 1035–1039, 1990.

[23] N. Acir, "A modified adaptive IIR filter design via wavelet networks based on Lyapunov stability theory," *Neural Comput. Appl.*, vol. 17, no. 5–6, pp. 463–469, 2008.

[24] S. G. Mc Sweeney and W. M. D. Wright, "Real time adaptive parametric equalisation of ultrasonic transducers," in *Proc. IEEE Ultrasonics Symp.*, 2009, pp. 2008–2010.

[25] S. G. Mc Sweeney and W. M. D. Wright, "Ultrasonic transducers," provisional U.S. patent application 61/102 946 Oct. 30, 2008, European patent application 08105496.7, Sep. 18, 2009.

[26] R. C. Eberhart and Y. Shi, "Particle swarm optimization: Developments, applications and resources," in *Proc. IEEE Int. Conf. Evolutionary Computation*, 2001, vol. 1, pp. 81–86.

[27] R. E. Kennedy, "Particle swarm optimization," in *Proc. IEEE Int. Conf. Neural Networks*, 1995, vol. 4, pp. 1942–1948.

[28] I. C. Trelea, "The particle swarm optimization algorithm: Convergence analysis and parameter selection," *Inf. Process. Lett.*, vol. 85, no. 6, pp. 317–325, 2003.

[29] S. Winder, *Analog and Digital Filter Design*, 2nd ed., Burlington, MA: Newnes, 2002, pp. 47–54.

[30] W. M. D. Wright, O. M. Doyle, and C. T. Foley, "Multi-channel data transfer using air-coupled capacitive ultrasonic transducers," in *Proc. IEEE Ultrasonics Symp.*, 2006, pp. 1805–1808.

[31] B. Birge, "PSOt—A particle swarm optimization toolbox for use with Matlab," in *Proc. IEEE Swarm Intelligence Symp.*, 2003, pp. 182–186.

[32] M. Clerc and J. Kennedy, "The particle swarm—Explosion, stability, and convergence in a multidimensional complex space," *IEEE Trans. Evol. Comput.*, vol. 6, no. 1, pp. 58–73, 2002.

Authors' photographs and biographies were unavailable at time of publication.